FEATURE

Shape Change Actuation for Precision Attitude Control

An air spindle testbed for experimental investigation.

By Dennis S. Bernstein, N. Harris McClamroch, and Jinglai Shen

The dynamics and control of spacecraft have been widely studied because of their technological significance [1]–[3]. For single-axis rotation, a rigid spacecraft can sometimes be viewed as a double integrator with torque input [4]. Three-dimensional rotation is more complex and involves three-axis torque inputs provided by thrusters with attitude and rate sensing. The problem becomes more difficult if fewer than three thrusters are available [5]–[7]. It is usually assumed that the mass distribution, and, thus, the inertia matrix, of the spacecraft is known, although robust and adaptive methods can be used when the inertia is uncertain [8].

Alternatively, control torques can be provided by reaction and momentum wheels, in which case the spacecraft mass distribution is constant despite the presence of moving components [9]. Many spacecraft use control moment gyros, which involve momentum wheels spinning at a constant rate and whose axis of rotation can be controlled through a single- or double-gimbal mechanism [10].

Although both thrusters and wheels can be used to apply control torques to the spacecraft, they play very dif-

0272-1708/03/$17.00©2003IEEE

ferent roles. Specifically, thrusters can change the angular momentum of the spacecraft, whereas wheels cannot, since total angular momentum is conserved. On the other hand, a momentum wheel can store momentum, whereas a thruster cannot. This distinction is critical since external disturbance torques must be counteracted through momentum dumping, for which thrusters are often utilized. However, thrusters require fuel, which must be brought from Earth and is limited, while wheels require electric power, which can be obtained from solar energy and, thus, is unlimited. Besides thrusters and wheels, alternative attitude control devices exploit gravity gradient and magnetic torques for stabilization, momentum dumping, and compensation of atmospheric drag, solar pressure, and other disturbance torques.

Returning to the dynamics of the spacecraft, it is important to keep in mind that most spacecraft are not monolithic rigid bodies, but rather consist of moving components such as spinning rotors for stabilization (as in a dual-spin spacecraft with a despun platform) and articulated appendages (solar panels, robotic arms, antennas, and instrument booms). In addition, the dynamics of large flexible appendages [11] and on-board fuel [12] can be excited by control actuators, thereby degrading the performance of the attitude control system. Flexible dynamics can also be excited by environmental disturbances such as heating and cooling.

This article focuses on an alternative technology for attitude control called *shape change actuation and control*. For a multibody spacecraft, that is, a spacecraft consisting of multiple rigid bodies connected by hinge, rotary, or prismatic joints, the spacecraft attitude dynamics are coupled with the shape dynamics that arise due to changes in the mass distribution. The objective is to control the spacecraft attitude by purposefully changing the mass distribution of the spacecraft [11], [13], [14]. Shape change actuation and control is not useful for momentum dumping or storage. Rather, it is intended for efficient, low-authority attitude control, possibly as a backup for thrusters and reaction wheels.

We describe the development of a multibody attitude control testbed for investigating and demonstrating shape change actuation. This testbed is based on an air spindle to allow low-friction, single-degree-of-freedom rotational motion. The article emphasizes the conceptual formulation of the problem, the design issues that were addressed in the development of the testbed, and the expected and unexpected issues that arose in the experimental investigation. The theoretical background for shape change actuation and control is not addressed, but references are given to relevant publications where this background is developed.

The attitude control problem for the platform supported by the air spindle and the proof masses is expressed in terms of a model that assumes conservation of angular momentum about the air spindle axis. Assuming that the angular momentum is exactly zero, a standard nonlinear drift-free control model is obtained that relates the two proof mass velocities, viewed as input variables, to the rate of change of the three configuration variables, namely the platform attitude and the positions of the proof masses. This model has the form of a nonholonomic control system. A survey of research on nonholonomic control systems, prior to 1995, is available in [15]. With the notable exception of control research on wheeled vehicles [15], there have been relatively few practical assessments of nonholonomic control approaches based on careful experimentation. One of our objectives is to provide such an assessment for spacecraft applications.

The testbed is based on an air spindle to allow low-friction single-degree-of-freedom rotational motion.

In the next section, we describe the design and development of the hardware for the experimental testbed. This section provides an experiment design case study in terms of the rationale for various design decisions and the constraints of time, money, physical limitations, and incomplete information. We discuss the shape-change attitude control problem for the air spindle testbed from a conceptual point of view. We present the basic air spindle testbed model, and we provide a description of several air spindle control strategies including open-loop and feedback controllers.

In subsequent sections we describe the controllers used in the experiments, and we report the results of control experiments using an open-loop controller and two different feedback controllers. In the latter sections we discuss differences between the experimental results and the expected results based on control analysis and simulation. A key modeling assumption is that the air spindle platform is level, and we describe our efforts to level the platform. In these sections, we also summarize what we learned from designing and operating the testbed from a hardware point of view, and we discuss the ramifications of the experiments for motivating new problems and research questions in control theory.

Hardware Development of the Air Spindle Testbed

In this section, we describe the hardware for the experimental setup, including the air spindle testbed, the real-

time control and communication system, and the actuator and power systems.

The testbed consists of a single-axis rotational platform controlled by translational shape change actuation; a schematic top-view diagram is shown in Figure 1. To satisfy the assumption that the total angular momentum is conserved and is zero, the platform should not be influenced by external moments, such as those due to friction and gravity. To achieve this objective, the air spindle is supported by a precision air bearing that supports the rotating elements by a thin film of air.

To take full advantage of the low friction of the air spindle, the control system should operate completely untethered to the room. This requirement implies that 1) all power for the control system is located on the platform, 2) all processing takes place on board the platform, and 3) all communication with the control processor is wireless. A data link with sufficient speed so that the control processor could be located off the platform was considered. However, this arrangement necessitates more complicated signal interfaces on the platform. We thus opted for an embedded processor with a relatively low-speed data link, as described below.

Since air spindle components are separated by a film of air, one might expect that the rotor and stator of the air spindle are capable of relative motion in translation and rotation along axes other than the desired rotation axis. In fact, a typical air spindle is extremely stiff to stator/rotor relative displacement in the presence of lateral forces as well as tilt in the presence of moments. This stiffness assures that the mounting platform does not tilt as the location of the center of mass varies during the experiment. However, as will be seen, the leveling of the platform itself is a limiting factor in the experiments.

The air spindle we chose is the model 4R Block-Head manufactured by Professional Instruments, Inc., Hopkins, Minnesota. The 4R Block-Head is extremely stiff to lateral forces and moments. To provide an experimental testbed, we specified the following items: 1) a base with adjustable tilt, 2) an encoder for measuring attitude, and 3) a mounting platform. For leveling the base, we specified adjustable feet, which are described later.

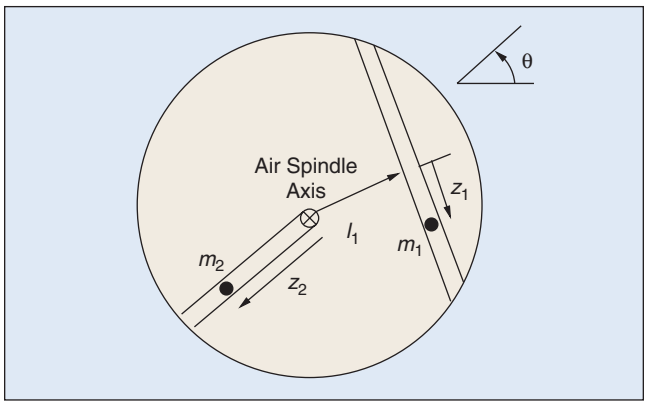

Figure 1. *Schematic of the top view of the air spindle testbed. Two proof masses are velocity-commanded to move along fixed linear tracks. In the absence of platform tilt, total angular momentum is conserved.*

Professional Instruments, Inc., routinely uses optical encoders for measuring the air spindle angle. However, these encoders are typically mounted so that the encoder signal is available in the nonrotating room frame. In our case, though, we require that the encoder signal be available in the rotating frame so that the on-board processor can use the rotation angle for feedback control. To this end the encoder is mounted in a reverse manner so that the wiring to the encoder rotates with the platform. Choosing a Heidenhain Corp., Schaumburg, Illinois, encoder model 1384, a glass encoder disk is mounted to the air spindle stator, while the scanning unit is mounted to the rotor. These components are noncontacting and thus frictionless. The signal wire from the scanning unit passes through the air spindle and through the center of the platform.

The encoder signal is processed by a multiplier circuit to provide 200,000 points per revolution, for an effective angular resolution of 6.5 arc s. Note that this specification does not imply that the accuracy of the encoder is 6.5 arc s; however, resolution and repeatability, which are features of optical encoders, are the specifications of relevance to our experiments [16].

Specification of the platform includes its shape, size, and thickness. We opted for a square platform to simplify the mounting of components. As to the size of the platform, we realized that control authority increases as the distance of the proof mass slots from the rotational center increases. On the other hand, a larger platform has greater inertia (in fact, the inertia increases as the fourth power of its dimension, making this an extremely sensitive specification), while increased inertia tends to decrease the authority of the shape change actuation. An additional difficulty was the fact that the processor dimensions and mass as well as the proof mass actuator stroke, force, and mass were not yet determined. Although it would have been desirable to design all system components simultaneously, the lead times were such that this was not possible. Using estimates of the proof mass actuator properties, we arrived at a specification of 15 in by 15 in for the platform.

To guarantee the performance of the air spindle, it is extremely important that the platform not deform so that the air spindle rotor does not deform. The least thickness that guarantees air spindle performance is 3/8 in stainless steel. Alternative designs involving a built-up platform of, for example, a thicker, smaller platform supporting a thin aluminum platform were also considered but not pursued. Our platform was machined with 1/4-20 through holes in a

1-in grid to allow mounting of components above and below the platform.

For real-time on-board processing, we use an embedded processor developed by Quanser Consulting, Toronto, Canada. This processor is based on a 586 processor with a 4 GB solid-state hard disk and a multi-Q I/O board allowing eight analog-to-digital (A/D) channels, eight digital-to-analog (D/A) channels, and eight encoder channels. The choice of processor was driven by the need to avoid a cooling fan, which would have adversely affected the air spindle dynamics. The A/D and D/A channels have a resolution of 13 bits over a ± 5 V range. The A/D sampling occurs sequentially with an acquisition time of 20 μs per channel, while the D/A latency is 5 μs per channel. The operating system is based on the Quanser Consulting WinCon real-time controller, which is compatible with the MathWorks Real-Time Workshop for implementing controllers programmed in Simulink. Communication with the host PC for experiment monitoring, parameter modification, and data acquisition is accomplished through a wireless ethernet connection. Power for the processor is provided by a 12 Vdc, 5 A-h notebook battery, which provides approximately one hour of operating time.

For shape change actuation, we use a pair of linear proof-mass actuators custom built by Planning Systems, Inc., Melbourne, Florida. Each actuator has a 1.73-lb moving magnet/linear bearing assembly as its proof mass with 5.5 in end-to-end travel. A U-channel linear motor made by Aerotech, Inc., Pittsburgh, Pennsylvania, model BLMUC-79, is the drive component of the actuator. An integrated Renishaw, Inc., Hoffman Estates, Illinois, linear encoder measures proof mass position with a resolution of 1 μm. Each actuator is driven by a model ASP-180-10 Accelus amplifier manufactured by Copley Controls Corp., Canton, Massachusetts. The amplifier is capable of 6 A continuous and 18 A peak. The amplifier parameters can be fully programmed by a PC through an RS-232 link and has self-tuning capability. With these components each actuator is capable of 5 lb continuous and 15 lb peak force. Power for the linear actuators is provided at 36 VDC by three 12-V lead acid batteries rated at 2.0 A-h. The 12-V batteries are mounted on the linear actuators to increase the amount of moving mass; the total moving mass is 0.16 slug. A photograph of the testbed layout can be seen in Figure 2.

Formulation of the Shape-Change Actuation and Control Problem

Air Spindle Model

Since our goal is to investigate shape change actuation and control, we consider the simplest problem involving a single unactuated rotational degree of freedom of the platform with two actuated proof masses that can translate along fixed, straight tracks. As shown in Figure 1, the offset, that is, the perpendicular distance from the platform axis to the proof mass track of the first proof mass, is positive, while the offset of the second proof mass track is zero, that is, the second track is aligned to intersect the air spindle axis. This layout for the proof masses characterizes the physical setup in our laboratory; our subsequent analysis will be for this particular case, although the results can be extended to the case in which both proof mass offsets are positive. This particular layout for the proof mass actuators was selected to achieve a large change in the platform and proof mass inertia about the air spindle axis, with the expectation that this arrangement would lead to improved control authority for the platform attitude. As shown subsequently, the angle between the proof mass tracks is irrelevant for control of the platform attitude.

The control objective is to use the two actuated proof masses to induce a desired attitude change of the platform. In particular, it is desired that a specified attitude change be made in the platform while the two proof masses eventually come to rest at specified locations. Thus, simultaneous position control of the platform attitude and the two proof masses is desired. The challenge of accomplishing this objective is due to the fact that there are only

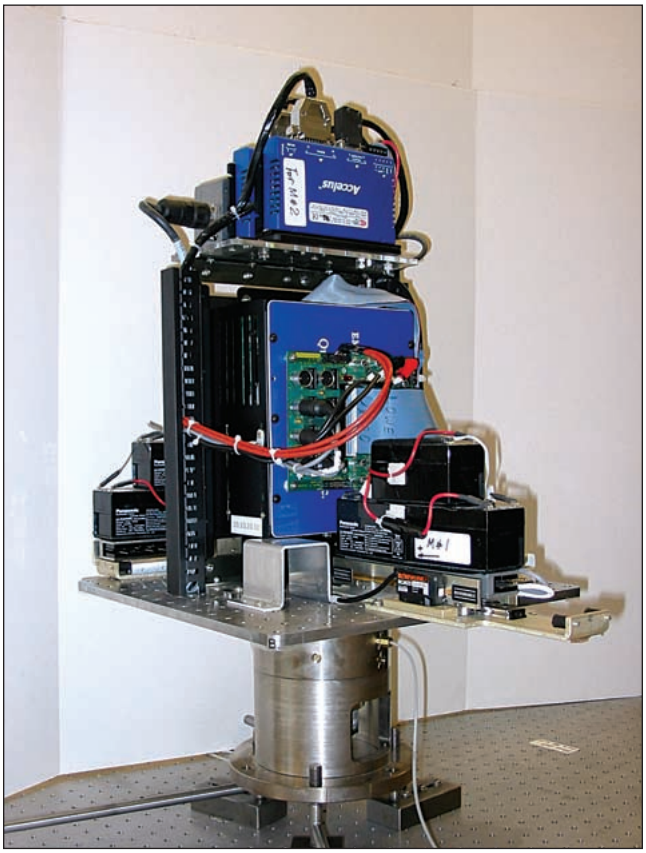

Figure 2. *Photograph of the air spindle testbed. A pair of proof mass actuators are mounted on a rectangular platform in accordance with the arrangement shown in Figure 1.*

two control inputs, namely, the two proof mass velocities, while we seek to control three degrees of freedom.

Our subsequent analysis is based on the assumption that there is no friction in the air bearing, air drag is negligible, and the platform is exactly leveled so there is no gravity moment about the air spindle axis. These assumptions imply that the total angular momentum is conserved. Moreover, if the system is initially in equilibrium, then the total angular momentum is identically zero.

Equations of Motion

In this section, we derive the equations of motion for the air spindle with two proof mass actuators. We first introduce the following notation:

I = the inertia of the platform including all components rigidly mounted on the platform;
θ = the attitude angle of the platform;
m_i = the mass of the ith proof mass, $i = 1, 2$;
z_i = the relative position of the ith proof mass with respect to a platform-fixed rotating frame, $i = 1, 2$.

As shown in Figure 1, we choose $z_1 = 0$ to correspond to the position along the first actuator axis whose distance to the rotation axis of the platform is minimized; this minimal distance is l_1. Since the offset of the second proof mass is zero, $z_2 = 0$ corresponds to the location of the platform rotational axis.

Based on the assumption that the total angular momentum is identically zero, it is shown in [17] that

$$\dot{\theta} = \frac{m_1 l_1 \dot{z}_1}{J + m_1 z_1^2 + m_2 z_2^2}, \tag{1}$$

where $J = I + m_1 l_1^2$. Let the control inputs u_i be the proof mass velocities $\dot{z}_i$, that is, $\dot{z}_i = u_i$. Then (1) can be expressed in a standard nonlinear form, affine in the controls, given by

$$\dot{z}_1 = u_1, \tag{2}$$
$$\dot{z}_2 = u_2, \tag{3}$$
$$\dot{\theta} = \frac{m_1 l_1 u_1}{J + m_1 z_1^2 + m_2 z_2^2}. \tag{4}$$

The nonlinear control systems described in (2)–(4) have no drift terms. It is easily seen that if the control variables are identically zero, the air spindle testbed is in equilibrium for every value of the platform angle and proof mass positions. It is easy to check that the linearized system is not controllable at any equilibrium.

The physical values of the parameters in the model are obtained from direct measurement or system identification:

$$m_1 = m_2 = 0.16 \text{ slug}, \quad l_1 = 6 \text{ in},$$
$$J = 45.8 \text{ slug-in}^2.$$

Control Problems

Controllability at an equilibrium of (2)–(4) is assessed by checking the Lie algebraic rank condition [18]. It can be verified that the two control vector fields and the first order Lie bracket of these two control vector fields span $\mathbb{R}^3$ when evaluated at an equilibrium that does not satisfy $z_2 = 0$. Stroke limits on the testbed constrain the position of the second proof mass to be positive, that is, $z_2 > 0$. Thus, the air spindle testbed, based on the above analysis, is locally controllable in a neighborhood of every physically feasible equilibrium. See [17] and [19] for more details about the controllability analysis.

Three different controllers, one open loop and two feedback, were constructed and tested experimentally. Theoretical analysis of these controllers follows standard techniques for nonholonomic systems. Since it is not our objective to treat the theoretical issues here, we only briefly describe the conceptual basis for these controllers.

We first develop and test an open-loop controller. In this case, the proof mass velocity controls are selected to transfer the configuration variables from a specified initial equilibrium configuration $(z_{1d}, z_{2d}, \theta_0)$ to a desired equilibrium configuration $(z_{1d}, z_{2d}, \theta_d)$; these controls are computed as explicit time functions that achieve the desired platform rotation. The open-loop controllers are based on standard geometric phase ideas; details of this controller are given in [17].

For the two feedback controllers, the control inputs depend on measurements of the configuration variables. The control objective is to transfer an initial equilibrium configuration $(z_1(0), z_2(0), \theta(0))$ to a desired equilibrium configuration $(z_{1d}, z_{2d}, \theta_d)$. The air spindle, described by (2)–(4), does not satisfy the Brockett necessary conditions for the existence of a smooth stabilizing controller. Various types of nonsmooth feedback controllers could be utilized; see [15] for a review of different control approaches. In our experiments, we used two different nonsmooth feedback controllers. The first is based on a hybrid switching scheme [20]. The second nonsmooth feedback control is based on a time and state transformation approach, introduced in [21].

As described previously, the proof mass velocities are viewed as control inputs. However, the physically implementable controls are the voltages to the proof mass amplifiers, which provide regulated currents to the linear proof mass actuators. Thus a nonlinear PD regulation controller is designed so that each proof mass actuator tracks the desired velocity commands. These regulators define an inner control loop for each actuator.

Experiments have demonstrated that each proof mass actuator acceleration can be adequately described by a deadzone type equation

$$\ddot{z} = \begin{cases} 105(v - v_d), & v > v_d, \\ 0, & -v_d \le v \le v_d, \\ 105(v + v_d), & v < -v_d, \end{cases} \tag{5}$$

where $\ddot{z}$ is the acceleration of the proof mass in in/s^2, v is the control voltage to the proof mass amplifier, which can vary from –5 V to +5 V, and v_d specifies the deadzone parameter. The deadzone effect is due to static friction between the proof mass actuator and its track. However, the deadzone width changes with proof mass position, varying from 0.2 V to 0.27 V. A feedback regulation controller has been designed for each proof mass actuator. The regulator control consists of a proportional-derivative part dependent on the proof mass command error and a deadzone compensator. Define the proof mass position error $e_z = z - z_d$, where z_d is the proof mass position command. The controller has the form

$$v = v_{dzc} + v_{pd},$$

where v_{dzc} is the dead-zone compensation part given by

$$v_{dzc} = \begin{cases} 0.24, & 50e_z < -0.24, \\ -50e_z, & -0.24 \le 50e_z \le 0.24, \\ -0.24, & 50e_z > 0.24, \end{cases}$$

and v_{pd} is the proportional and derivative part that regulates the closed-loop transient dynamics given by

$$v_{pd} = \frac{1}{105}\left(k_p e_z + k_d \dot{e}_z\right).$$

Here k_p and k_d are control parameters defining the closed-loop dynamics. Experiments have demonstrated that this proof mass regulation controller works well for a variety of proof mass position commands.

Experimental Protocol

We briefly describe our experimental protocol. First, we place each proof mass at its initial position. We then level the air spindle platform as accurately as possible by manually adjusting the three legs on the air spindle base. This leveling is crucial to the experiments since an unleveled platform is strongly affected by gravity. The platform is brought to rest, which initializes the experiment.

In the following sections, we describe the controllers that have been experimentally tested. Experimental results are presented for each control strategy. In the subsequent sections, the experimental results are interpreted, especially in terms of the residual effects of imperfect leveling.

Geometric Phase Open-Loop Controller and Experimental Results

An open-loop controller is proposed, and experimental results are presented. The proof mass velocities are specified as an explicit time function that transfers an initial equilibrium configuration $(z_{1d}, z_{2d}, \theta_0)$ to a desired equilibrium configuration $(z_{1d}, z_{2d}, \theta_d)$ in a specified time period T. Note that the platform attitude changes but there is no net change in the proof mass positions.

The open-loop controllers are based on standard geometric phase ideas. An integration of (4) shows that periodic motions of the proof masses lead to a change in the platform angle; the proof mass periodic motions can be selected to achieve the desired change in the platform. The details for this controller construction are given in [17].

The particular controller used in the experiments is given by

$$u_1(t) = |\alpha| \sin\left(\frac{2\pi t}{T}\right), \quad u_2(t) = \alpha \cos\left(\frac{2\pi t}{T}\right), \tag{6}$$

where $t \in [0, T]$ The resulting change of θ can be expanded as a series [22]

$$\Delta\theta = \theta(T) - \theta_0 2\pi \left[\text{sign}(\alpha) \sum_{n=1}^{\infty} C_n \left(\frac{T|\alpha|}{2\pi}\right)^{n+1} \right], \tag{7}$$

where $(T|\alpha|/2\pi)$ is assumed to be chosen such that this series is convergent, and the coefficients C_n are given by

$$C_n = \begin{cases} \sum_{i=0,2,\cdots,n-1} \Delta F^{(n,i)} A_n^i, & \text{if } n \text{ is odd}, \\ \sum_{i=1,3,\cdots,n-1} \Delta F^{(n,i)} A_n^i, & \text{if } n \text{ is even}, \end{cases}$$

and

$$\Delta F^{(n,i)} = \frac{\partial^n f_1(z)}{\partial z_1^i \partial z_2^{n-i}}\Big|_{z=(z_{10}, z_{20})},$$

$$A_n^i = \begin{cases} \dfrac{(n+i)(n+i-2)\cdots 1}{(n+1)!\,i!}, & \text{if} \quad i = n-1, \\ \dfrac{(n+i)(n+i-2)\cdots 1}{(n+1)!\,i!(n-i-1)(n-i-3)\cdots 2}, & \text{if} \quad i \le n-3, \end{cases}$$

where $f_1(z) = (m_1 l_1/J + m_1 z_1^2 + m_2 z_2^2)$ and (z_{10}, z_{20}) is the initial condition of (z_1, z_2).

The scalar parameter α is determined to achieve the desired platform attitude change in the specified time period. As shown in [22], α can be determined by numerically solving a root-finding problem for the desired platform attitude change.

The initial angle is $\theta_0 = 0^\circ$, and the desired platform attitude in one period is $\theta_d = 1^\circ$. The frequency of the proof mass motions is chosen as 0.25 Hz (or equivalently $T = 4$ s). Experiments are performed with $z_1(0) = z_{1d} = 0$ in and $z_2(0) = z_{2d} = 7$ in. The control parameter is $\alpha = \pi$, which corresponds to sinusoidal proof mass motions with an amplitude of 2 in.

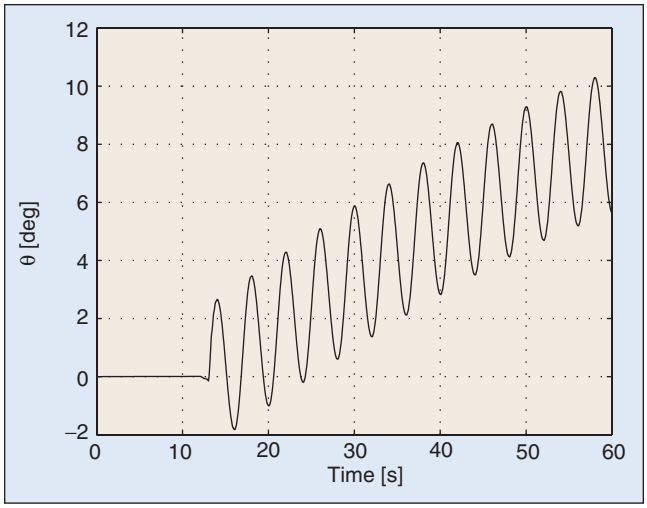

Figure 3. *Platform attitude response using the geometric phase open-loop controller. These experimental results illustrate the rotational drift due to periodic proof mass motion.*

Experimental results are shown in Figures 3 and 4, which show typical time responses for the platform rotation. The control inputs are repeated over several periods to show the drift in the average value of the platform attitude. Experimental results and simulation results (not shown) are in close agreement. This agreement provides good evidence that the constructed control model and the control strategies are accurate representations of the controlled air spindle testbed, at least for a time interval of operation of 50 s.

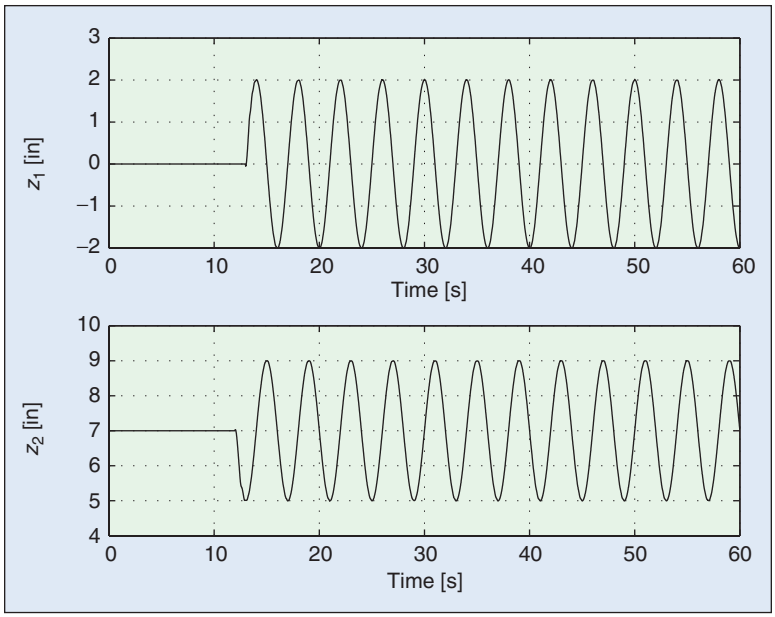

Figure 4. *Proof mass position responses using the geometric phase open-loop controller. The experimental results are based on sinusoidal proof mass motion.*

Hybrid Feedback Controller and Experimental Results

We now present a feedback controller that asymptotically transfers an initial equilibrium configuration $(z_1(0), z_2(0), \theta(0))$ to a desired equilibrium configuration $(z_{1d}, z_{2d}, \theta_d)$. This feedback controller is based on an iterative application of the geometric phase open-loop controller given in (6). This approach, which was originally developed for a class of nonlinear cascade systems in [20], leads to a hybrid control structure that involves continuous feedback of the proof mass position errors, periodically sampled feedback of the platform angle error, and gain adaptation. Details of the controller design procedure are given in [20].

The particular hybrid controller structure used in the experiments is given by

$$u_1(t) = -k_1(z_1 - z_{1d}) + |\alpha_k| \sin\left(\frac{2\pi t}{T}\right), \quad kT \le t \le (k+1)T, z \tag{8}$$

$$u_2(t) = -k_1(z_2 - z_{2d}) + \alpha_k \cos\left(\frac{2\pi t}{T}\right), \quad kT \le t \le (k+1)T, \tag{9}$$

where α_k is a constant parameter during $kT < t \le (k+1)T$ that can be changed at $t = kT$. Let $0 < \gamma < 1$ and $\Delta\theta(t) = \theta(t) - \theta_d$. The choice of the parameter α_k is determined by the following algorithm:

i) If $z_1(0) = z_{1d}, z_2(0) = z_{2d}, \theta(0) = \theta_d$, set $\alpha_0 = 0$; otherwise, choose $\alpha_0 \neq 0$;
ii) If $\Delta\theta(kT) = 0$ or $\alpha_k \Delta\theta(kT) > 0$, set $\alpha_k = \alpha_{k-1}$;
iii) If $\alpha_k \Delta\theta(kT) \le 0$ and $\Delta\theta(kT) \neq 0$, then set $\alpha_k = \gamma |\alpha_{k-1}| \text{sign}(\Delta\theta(kT))$.

This hybrid feedback controller achieves asymptotic convergence of the closed-loop state errors to zero [20].

For the experiment, the desired equilibrium is

$$z_{1d} = 0 \text{ in}, \quad z_{2d} = 7 \text{ in}, \quad \theta_d = 0^\circ,$$

while the initial conditions are chosen as

$$z_1(0) = 0 \text{ in}, \quad z_2(0) = 7 \text{ in}, \quad \theta(0) = -1^\circ.$$

We choose the control gain $k_1 = 1 \text{ s}^{-1}$, the period $T = 2$ s, that is, $\omega = \pi$, the initial gain parameter $\alpha_0 = 2\pi$ in/s and $\gamma = 0.5$. Experimental results are shown in Figures 5 and 6. It can be seen in Figure 5 that the gain parameter α changes at $t = 2,\ 18,\ 32$ s, respectively. After 35 s, the states are very close to the desired equilibrium. The platform attitude gradually drifts away from the equilibrium, for reasons that are explained later.

Time-State Feedback Controller and Experimental Results

We now consider a feedback controller that asymptotically transfers an initial equilibrium configuration $(z_1(0), z_2(0), \theta(0))$ to a neighborhood of a desired equilibrium configuration $(z_{1d}, z_{2d}, \theta_d)$. This feedback controller is a time-state controller based on a control method for nonholonomic control systems developed in [23]–[27]. The key idea in this method is that a transformation is made to obtain time and state equations, with one of the original state variables serving as the independent variable (pseudo-time) for the state part. Controllers can be developed for the mode corresponding to increasing pseudotime and for the mode corresponding to decreasing pseudotime. Appropriate switching between these modes, and the introduction of a convergence mode, guarantees that the proof mass position and platform attitude errors asymptotically approach a small neighborhood of the origin.

The particular time-state controller used in the experiments is summarized as follows. Let $z_{i\min}$, $z_{i\max}$, $i = 1, 2$, denote the limits of the proof mass positions, and define

$$z_{2s} = z_{2\max} - z_{2\min}, \quad z_{2c} = \frac{z_{2\max} + z_{2\min}}{2}.$$

The subsequent controller is expressed in terms of the functions

$$V_f = \frac{1}{2}\xi_3^2 + \frac{1}{2k_{3f}^2}(\xi_2 + k_{3f}\xi)^2, \tag{10}$$

$$V_b = \frac{1}{2}\xi_3^2 + \frac{1}{2k_{3b}^2}(\xi_2 - k_{3b}\xi_3)^2, \tag{11}$$

where k_{3f} and k_{3b} are positive constants, and

$$\xi_2 = \frac{z_{2s}}{\pi}\left(\tan\frac{\pi(z_2 - z_{2c})}{z_{2s}} - \tan\frac{\pi(z_{2d} - z_{2c})}{z_{2s}}\right), \tag{12}$$

$$\xi_3 = \theta_d - \theta + \frac{m_1 l_1}{\sqrt{m_1(J + m_2 z_{2d}^2)}} \times\left\{\tan^{-1}\left(\sqrt{\frac{m_1}{J + m_2 z_{2d}^2}}z_1\right) - \tan^{-1}\left(\sqrt{c\frac{m_1}{J + m_2 z_{2d}^2}}z_{1d}\right)\right\}. \tag{13}$$

Next, let ε, ε_s be small positive constants and let $k_1 > 0, k_2 > 0$. Choose z_1 as pseudo-time variable. There are three control modes for which switching logic is given by the following algorithm:

i) If $t = 0$ or $z_1 - z_{1\min} < \varepsilon_s$, then use
$u_1 = -k_1(z_1 - z_{1\max}), \quad u_2 = -k_2(\xi_2 + k_{3f}\xi_3)$,
until $z_1 - z_{1\max} > -\varepsilon_s$.

ii) If $z_1 - z_{1\max} > -\varepsilon_s$, then use
$u_1 = -k_1(z_1 - z_{1\min}), \quad u_2 = -k_2(\xi_2 - k_{3b}\xi_3)$,
until $z_1 - z_{1\min} < \varepsilon_s$.

Our control experiments confirm the feasibility of using two proof mass actuators (shape-change actuation) to achieve platform attitude maneuvers.

iii) If either of the following cases holds

$$z_1 > z_{1d}, \ V_b < \varepsilon \quad \text{or} \quad z_1 < z_{1d}, \ V_f < \varepsilon,$$

then

$$u_1 = -k_4(z_1 - z_{1d}), \quad u_2 = -k_4(z_2 - z_{2d}).$$

This control strategy achieves convergence to a sufficiently small neighborhood of the desired equilibrium $(z_{1d}, z_{2d}, \theta_d)$ defined by the constant ε.

The time-state controller has been implemented on the air spindle testbed. The desired equilibrium is

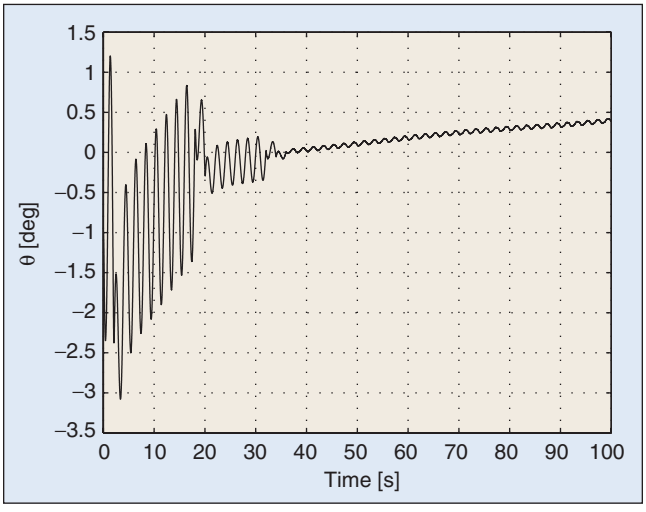

Figure 5. *Platform attitude response using the hybrid controller. These experimental results involve iterative application of the geometric phase controller with varying amplitude. The residual drift is due to imperfect leveling of the platform.*

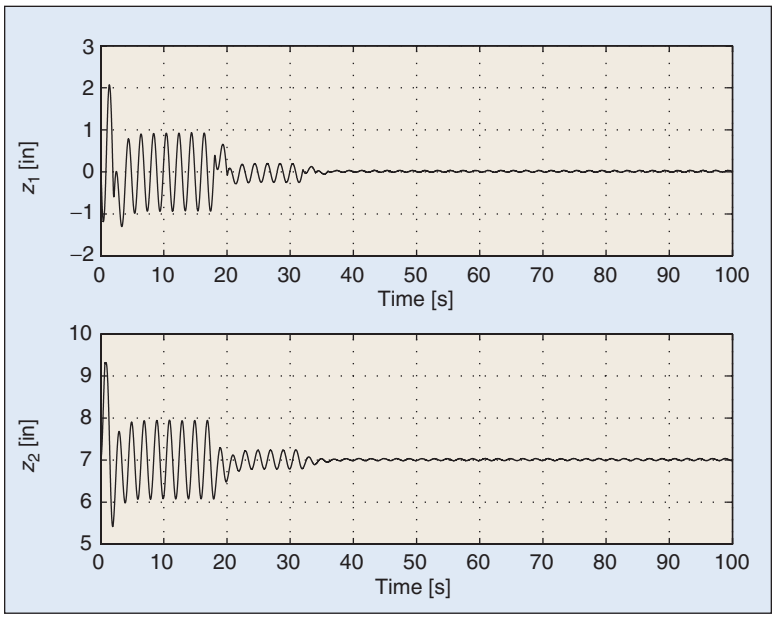

Figure 6. *Proof mass position responses using the hybrid controller. The proof mass motion corresponds to the platform rotation shown in Figure 5.*

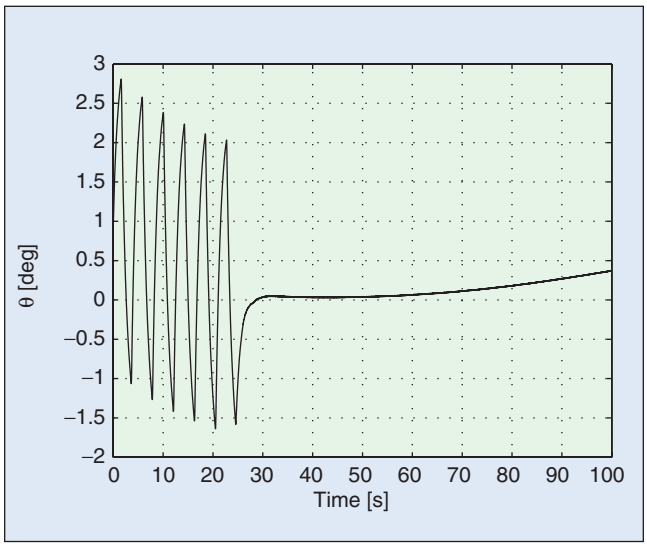

Figure 7. *Platform attitude response using the time-state controller. The controller uses the position z_1 of the first proof mass actuator as the pseudo-time variable.*

$$z_{1d} = 0 \text{ in}, \quad z_{2d} = 7 \text{ in}, \quad \theta_d = 0^\circ$$

and the initial conditions are

$$z_1(0) = 0 \text{ in}, \quad z_2(0) = 7 \text{ in}, \quad \theta(0) = 1^\circ.$$

The proof mass stroke parameters for our experimental tests are

$$z_{1\max} = 2 \text{ in}, \quad z_{1\min} = -2 \text{ in},$$
$$z_{2s} = 4 \text{ in}, \quad z_{2c} = 7 \text{ in}$$

and

$$k_1 = 1 \text{ s}^{-1}, \quad k_2 = 10 \text{ s}^{-1},$$
$$k_{3f} = k_{3b} = 50 \text{ in}, \quad k_4 = 1 \text{ s}^{-1},$$
$$\varepsilon = 10^{-6}, \quad \varepsilon_s = 0.5 \text{ in}.$$

Experimental results are shown in Figures 7 and 8. It can be seen that, after 30 s, the states are close to the desired equilibrium. The platform attitude gradually drifts away from the equilibrium; this behavior is explained in a later section.

Interpretation of the Experimental Results

We now interpret the experimental results obtained in light of the relevant nonlinear control theory. We first compare the open-loop control responses with the feedback control responses and then compare the two sets of feedback responses. Limitations of the results are indicated, and suggestions are made about open research issues.

It is clear that the responses for the open-loop controller are much faster than the responses for the feedback controller. The open-loop controller is designed for the specific initial conditions used in the experiment. For that initial condition, the control input is designed to have high control authority. On the other hand, the two feedback controllers are designed for a range of initial conditions of which experimental results are shown only for the indicated initial conditions. This difference in design specifications leads to the differences in the open-loop responses and the feedback responses.

The experimental responses for the two feedback controllers are comparable, with the time-state controller providing slightly faster response than the hybrid controller. In each case, the errors are reduced to near zero, for the selected initial conditions, in approximately 30 s. Each method requires the selection of gain parameters. The controllers that we used in the experiments have not been optimally tuned for the fastest possible responses. Rather, the experimental results are suggestive of the time response properties for this particular experimental setup.

There are two important sets of constraints that are relevant in this experiment. There are state constraints due to stroke limits on the proof masses and control constraints that arise from bandwidth limitations of the proof mass actuators. The controllers used in the experiments were designed in an ad hoc way to satisfy these constraints.

It is easy to make arbitrary changes in the equilibrium values of the two proof mass positions, since these are directly actuated. It is much more difficult, as we have shown, to change the platform attitude with zero net change in the proof mass positions. In each of the experiments, a 1° change in the platform is commanded, and the experimental results demonstrate that such changes can be achieved. If a larger change in the platform attitude is commanded, then a sequence of successive incremental changes can be commanded using the same controllers in a repetitive fashion.

The experimental responses demonstrate that the feedback controllers can compensate for an initial platform attitude error. The nonlinear control theory suggests, and our experiments confirm, that the controllers are not sensitive to small errors in the platform inertia or in the proof mass values. However, the feedback controllers cannot compensate for persistent moment disturbances since these disturbances destroy the equilibria of the platform. In our experiments, the most important disturbance, or model error, arises from the fact that the platform is not exactly horizontal so that small gravity moments in fact act on the platform.

Effects of Gravity on the Experimental Results

In this section, we describe our investigation of experimental errors that are evident from the differences in the experimental responses and the responses that we expect based on theoretical analysis and simulations. We show that platform tilt, and the associated gravity effects, is the most important source of experimental error. Since it is not our goal to control a tilted air spindle, we have to eliminate gravity effects due to the tilt as much as possible. However, in spite of our efforts to level the platform, the experimental results reflect the fact that the platform is not perfectly level. We point out how these effects influence the controlled responses of the platform angle.

Although there is generally good agreement between the experimental platform angle responses and the simulated platform angle responses, this agreement is restricted to relatively short time periods on the order of a minute. For longer time periods, there is divergence between the responses. We undertook a systematic investigation to explain and reduce the sources responsible for the theoretical and experimental response differences. Several possibilities were suggested, namely, 1) ambient floor vibrations, 2) ambient room air currents, and 3) air spindle tilt. Although air spindle tilt was the most obvious source, it was clear that other effects were present. Specifically, we observed that the platform tended to oscillate with increasing amplitude, suggesting forcing from sources other than gravity.

The air spindle was originally mounted on a low-mass optical table that vibrated due to ambient floor vibrations. We thus relocated the testbed to a high-mass table, and air spindle accelerations were significantly reduced. Nevertheless, oscillations of increasing magnitude continued to be observed, suggesting forcing from air currents. To address this problem, we built an acrylic box to house the entire experiment. Nevertheless, the effects persisted, and we conjectured that the disturbance was due to asymmetric air flow inside the air spindle itself. However, engineers at Professional Instruments assured us that the air spindle was designed so that the internal air flow produced virtually zero net moment, to the extent that a carefully mounted, undisturbed air spindle could detect the rotation of the Earth. We soon discovered that the vented air outflow from the air spindle was forcing the air spindle; routing the outflow eliminated that disturbance source.

Having reduced ambient vibrations and internal and external air flow as major disturbance sources, the key remaining source of disturbance was the moment due to gravity. Of course, the effect of gravity is zero if the center of mass is precisely located at the rotational center, and this is true even if there were runout between the platform and spindle. However, proof mass actuation necessitated that the center of mass not be fixed, and thus we

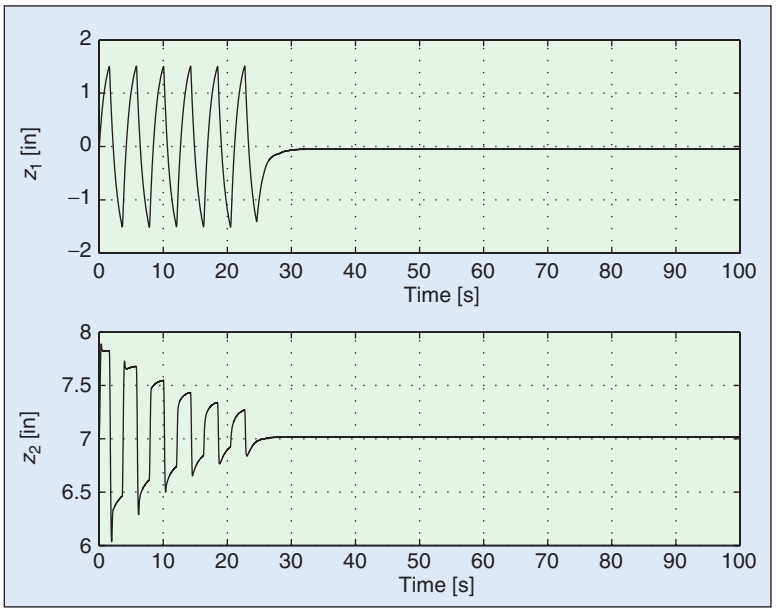

Figure 8. *Proof mass position responses using the time-state controller. Both proof mass actuators come to rest at the prescribed equilibrium positions.*

could at best hope to move the (variable) center of mass within the vicinity of the rotational center. Nonzero tilt of the air spindle platform gives rise to oscillatory pendulum dynamics of long period [28].

Our high-mass optical table has rigid legs, while the base of the air spindle is supported by three adjustable legs; see Figure 9. To reduce the tilt of the air spindle platform, we use a high sensitivity leveling mechanism. The three shafts were machined with threads of 1/2-13 on one end and threads of 1/2-20 on the opposite end. The lower end of each shaft is inserted into a tapped support block. By turning each shaft by means of a 12-in arm with an adjustment resolution of approximately 1°, the differential displacement provided by the shaft can be used to tilt the air spindle with a differential resolution of approximately 0.013°. This mechanism is crucial in reducing the platform tilt.

Unlike linear control systems, the class of systems studied in this article can be controlled only in a weak sense.

The air spindle model presented in (1) has been generalized by assuming that the platform is not exactly level, so there is a gravity moment that acts about the air spindle axis. Such a generalized model has been constructed and simulations have been developed. Experiments have been carried out to identify the parameters in this model; a typical estimated tilt angle is 0.015°. The details of the model and experimental results are given in [28]. This model demonstrates that the long-term experimental effects, which are not explained by the zero-tilt model used in this article, are explained by including gravity in the presence of platform tilt in the generalized model. For example, once the proof mass actuators are fixed, the tilted air spindle has pendulum-like dynamics around a stable equilibrium [28].

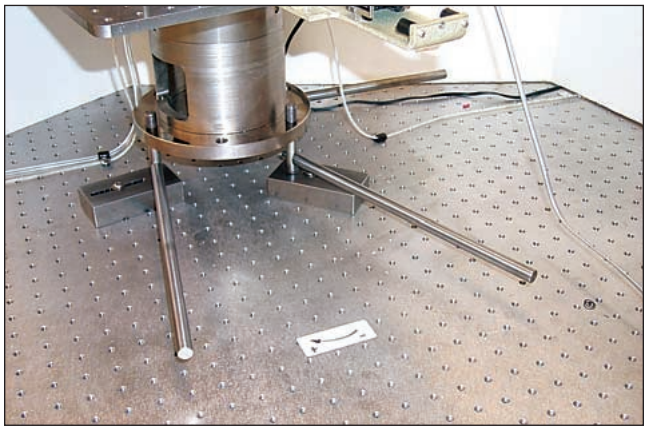

Figure 9. *Photograph of the air spindle supports. The 12-in arms are used to rotate the support shafts, which have differential screw threads for precise adjustments.*

The controllers used in the experiments are designed based on the assumption that there is no platform tilt, but our experiments make clear that even a small tilt angle of 0.015° significantly affects the control performance. For example, unlike the leveled model for which arbitrary platform attitude and proof mass positions can be an equilibrium, there exists only one stable platform attitude equilibrium for fixed proof mass positions when the platform is tilted. In the control design and experimental tests, more than 80% of the laboratory setup time is spent on leveling the platform, locating an equilibrium, and choosing appropriate initial conditions and control parameters to achieve satisfactory performance under the influence of gravity effects. We summarize our laboratory experiences in the subsequent paragraphs.

Due to the presence of platform tilt, our choice of controllers, control parameters, and initial conditions is restricted. A controller designed on the basis of the leveled model is effective for only a relatively short time period, about 50 s in the experimental platform attitude responses already presented. Thus convergence of the closed-loop responses, within this time period, is essential. As a consequence of this experimental constraint, we were unable to consider control methods, such as time-varying controllers, that have slower convergence rate. Furthermore, initial conditions were chosen to be close to an equilibrium to reduce gravity effects on platform attitude response.

Two issues were found to be important in the control experiments. First, fast convergence requires proof mass motions of large magnitude, but this may lead to difficulties in satisfying proof mass stroke and velocity limits. For example, the gains in the hybrid controller must be carefully selected to achieve fast convergence while not violating the stroke and velocity limits. Second, there is a tradeoff between convergence speed and control precision. For example, in the time-state controller, the tolerance parameter that determines when the terminal convergence mode is activated must be carefully selected. If this parameter is too small, convergence is slow and the platform tilt effects may dominate. On the other hand, control precision requires that this parameter should not be large.

We now summarize our evaluation of the two feedback control methods based on our laboratory experi-

ences. The hybrid controller is easy to design and implement. It is simple, depending on only three control gains and a frequency parameter. Our experiments indicate that it is robust to uncertainties in the platform inertia and proof mass values. But it is, of course, not robust to platform tilt. The control gains monotonically decrease, which provides guaranteed convergence, at least in the ideal case of a leveled platform. However, it also leads to slightly slower convergence, compared with the responses for the time-state controller.

The time-state controller is somewhat more complicated to design and implement. It involves seven control gains, and the switching logic is somewhat complex. Our experiments indicate that it is also robust to uncertainties in the platform inertia and proof mass values. But it is, of course, not robust to platform tilt. If the control gains are carefully chosen, the full stroke of the proof masses can be utilized resulting in relatively fast closed-loop responses.

Conclusions

We provided a summary of our experiences in developing and utilizing the air spindle testbed as an experimental facility for studying a physical implementation of a nonholonomic control system. Our original concept was that we could easily evaluate a variety of nonlinear controllers that have been proposed in the literature. In fact, the hardware acquisition and development time far exceeded what we had originally anticipated. More interestingly, we found that standard nonlinear controllers for nonholonomic systems, in the forms that appear in the published literature, could not be easily adapted to the experiments.

We spent much time on hardware development, attempts to level the platform to eliminate the effects of gravity, and on control design and redesign. We did not anticipate the difficulties in control design and experimental tests caused by gravity effects due to platform tilt. Experiments show that these effects are so crucial that they must be taken into account and handled in a careful way. Another practical design issue is the stroke and velocity limits on these proof mass actuators. The controllers that we evaluated in this article were tuned in an ad hoc way to include the effects of constraints, but we have subsequently developed systematic procedures for including these constraint effects in the controller design process [29].

It should also be mentioned that, unlike linear control systems, the class of systems studied in this article can be controlled only in a weak sense. In other words, the control authority for this class of nonlinear systems is intrinsically low. This feature is reflected in the nonlinear control analysis, and it is the source of many of the challenges that we faced in carrying out good control experiments.

The issues just described have motivated further work on the design of nonlinear controllers, of both the hybrid type and the time-state type. In particular, modifications have been made to those controllers to obtain higher controller authority using the full range of state and control constraints without violating the constraints. These modifications are beyond the scope of the present article.

Our reported control experiments clearly confirm the feasibility of using two proof mass actuators (shape-change actuation) to achieve platform attitude maneuvers, at least in the absence of gravity or gravity gradient effects. These results should not be viewed as definitive evaluations of the hybrid controller or the time-state controller methods. Although our experimental results are consistent with the available theory and with extensive computer simulations that we performed, the experiments did make clear to us that issues that we initially ignored, such as gravity effects due to platform tilt and proof mass stroke and velocity limits, are critical. The experiments raised these and other questions that provide motivation for continued research on dynamics and control via shape change actuation.

Acknowledgments

This research was supported in part by the Air Force Office of Scientific Research under grants F49620-01-1-0094 and F49620-99-1-0152 and the National Science Foundation under grants ECS-9729290, ECS-9906018, DMS-9803181, and ECS-0140053.

We wish to thank Prof. Mitsuji Sampei of Tokyo Institute of Technology for his help in developing the time-state controller. We also thank Jeff Perry of Professional Instruments, Jacob Apkarian of Quanser Consulting, Scott Greeley of PSI, Inc., Dean Crumlish of Copley Controls, and David McLean of the University of Michigan for valuable assistance.

References

[1] P.C. Hughes, *Spacecraft Attitude Dynamics*. New York: Wiley, 1986.

[2] T.R. Kane, P.W. Likins, and D.A. Levinson, *Spacecraft Dynamics*. New York: McGraw-Hill, 1983.

[3] M.H. Kaplan, *Modern Spacecraft Dynamics and Control*. New York: Wiley, 1976.

[4] V. Rao and D.S. Bernstein, "Naive control of the double integrator: A comparison of a dozen diverse controllers under off-nominal condi tions," in *Proc. Amer. Contr. Conf.*, San Diego, CA, 1999, pp. 1477–1481.

[5] H. Krishnan, N.H. McClamroch, and M. Reyhanoglu, "Attitude stabilization of a rigid spacecraft using two control torques: A nonlinear control approach based on the spacecraft attitude dynamics," *Automatica*, vol. 30, pp. 1023–1027, 1994.

[6] C.-J. Wan and D.S. Bernstein, "Rotational stabilization of a rigid body using two torque actuators," in *Proc. Conf. Decision and Control*, San Antonio, TX, 1993, pp. 3111–3116.

[7] C.-J. Wan and D.S. Bernstein, "Nonlinear feedback control with global stabilization," *Dynam. Contr.*, vol. 5, pp. 321–346, 1995.

[8] J. Ahmed, V.T. Coppola, and D.S. Bernstein, "Asymptotic tracking of spacecraft attitude motion with inertia identification," *AIAA J. Guid. Contr. Dynam.*, vol. 21, pp. 684–691, 1998.

[9] H. Krishnan and N.H. McClamroch, "Attitude stabilization of a rigid spacecraft using two momentum wheel actuators," *AIAA J. Guid. Contr. Dyn.*, vol. 18, pp. 256–263, Mar.-Apr., 1995.

[10] J. Ahmed and D.S. Bernstein, "Adaptive control of a double-gimbal control-moment gyro with unbalanced rotor," *AIAA J. Guid. Contr. Dynam.*, vol. 25, pp. 105–115, 2002.

[11] C. Rui, I. Kolmanovsky, and N.H. McClamroch, "Nonlinear attitude and shape control of spacecraft with articulated appendages and reaction wheels," *IEEE Trans. Autom. Contr.*, vol. 45, pp. 1455–1469, 2000.

[12] S. Cho, N.H. McClamroch, and M. Reyhanoglu, "Feedback control of a space vehicle with unactuated fuel slosh dynamics," in *Proc. AIAA Guid. Nav. Contr. Conf.*, Denver, CO, 2000.

[13] S. Cho, N.H. McClamroch, and M. Reyhanoglu, "Dynamics of multibody vehicles and their formulation as nonlinear control systems," in *Proc. Amer. Contr. Conf.*, Chicago, 2000, pp. 3908–3912.

[14] J. Shen and N.H. McClamroch, "Translational and rotational maneuvers of an underactuated space robot using shape change actuators," *Int.. J. Robot. Res.*, vol. 21, no. 5–6, p. 607–618, 2002.

[15] I. Kolmanovsky and N.H. McClamroch, "Developments in nonholonomic control problems," *IEEE Contr. Syst. Mag.*, vol.15, no. 6, pp. 20–36, Dec. 1995.

[16] D.S. Bernstein, "Sensor performance specifications," *IEEE Contr. Syst. Mag.,* vol. 21, pp. 9–18, Aug. 2001.

[17] J. Shen, N.H. McClamroch, and D.S. Bernstein, "Air spindle attitude control via proof mass actuators," in *Proc. Conf. Decision and Control*, Orlando, FL, 2001, pp. 4616–4621.

[18] H. Nijmeijer and A. van der Schaft, *Nonlinear Dynamical Control Systems*. New York: Springer-Verlag, 1990.

[19] J. Shen, "Nonlinear control of multibody systems with symmetries via shape change," Ph.D. dissertation, Univ. of Michigan, Dept. Aerospace Engineering, Ann Arbor, 2002.

[20] I. Kolmanovsky and N.H. McClamroch, "Hybrid feedback laws for a class of cascade nonlinear control systems," *IEEE Trans. Automat. Contr.*, vol. 41, pp. 1271–1282, Sept. 1996.

[21] M. Sampei, M. Ishikawa, and M. Koga, "Control of nonholonomic systems using time-state control form," in *Proc. TITech COE/Super Mechano-systems Workshop*, Japan, 1998, pp. 24–31.

[22] J. Shen and N.H. McClamroch, "Translational and rotational spacecraft maneuvers via shape change actuators," in *Proc. American Control Conf.*, Arlington, VA, 2001, pp. 3961–3966.

[23] H. Date, M. Sampei, D. Yamada, M. Ishikawa, and M. Koga, "Manipulation problem of a ball between two parallel plates based on time-state control," in *Proc. Conf. Decision and Control*, Phoenix, 1999, pp. 2120–2125.

[24] T. Nakagawa, H. Kiyota, M. Sampei, and M. Koga, "An adaptiveD-control of a nonholonomic space robot," in *Proc. Conf. Decision and Control*, San Diego, CA, 1997, pp. 3632–3633.

[25] M. Sampei, " A control strategy for a class of nonholonomic systems: time-state control form and its application," in *Proc. Conf. Decision and Control*, Orlando, FL, 1994, pp. 1120–1121.

[26] M. Sampei, H. Kiyota, M. Koga, and M. Suzuki, "Necessary and sufficient conditions for transformation of nonholonomic system into time-state control form," in *Proc. Conf. Decision and Control*, Kobe, Japan, 1996, pp. 4745–4746.

[27] M. Sampei, H. Kiyota, and M. Ishikawa, "Time-state control form and its application to a nonholonomic space robot," in *Proc. IFAC Symp. Nonlinear Control System Design*, 1995, pp. 759–764.

[28] J. Shen, N.H. McClamroch, and D.S. Bernstein, "Attitude control of a tilted air spindle testbed using proof mass actuators," in *Proc. American Control Conf.*, Anchorage, AK, 2002, pp. 934–939.

[29] M. Sampei, J. Shen, and N.H. McClamroch, "Feedback control of the air spindle system," in *Proc. American Control Conf.*, Denver, CO, 2003, pp. 483–488.

Dennis S. Bernstein is a faculty member in the Aerospace Engineering Department at the University of Michigan, where he teaches courses in classical and modern control theory, flight mechanics, and control of vibration and flow. His research interests include adaptive control and nonlinear identification with application to all areas of aerospace engineering.

N. Harris McClamroch is a professor at the University of Michigan. He has published papers in the areas of robustness, optimal control, estimation, stochastic control, and nonlinear control. He has worked on control engineering problems arising in flexible space structures, robotics, automated manufacturing, and aerospace flight systems. He is a Fellow of the IEEE, received the Control Systems Society Distinguished Member Award, and is a recipient of the IEEE Third Millennium Medal. He served as editor of *IEEE Transactions on Automatic Control* and as president of the IEEE Control Systems Society. He can be contacted at the Department. of Aerospace Engineering, 1320 Beal St., The University of Michigan, Ann Arbor, MI 48109, U.S.A., nhm@umich.edu.

Jinglai Shen is a postdoctoral research associate in the Department of Aerospace Engineering at the University of Michigan, Ann Arbor. He received his B.S.E. and M.S.E. degrees in automatic control from Beijing University of Aeronautics and Astronautics, China, in 1994 and 1997, respectively, and his Ph.D. degree in aerospace engineering from the University of Michigan, Ann Arbor, in 2002. His research interests include dynamical systems, nonlinear control, geometric approaches in mechanics and control, and control of multi-agent and hybrid systems with applications to aerospace systems, robotic systems, and other physical or man-made systems. He is an associate member of the IEEE.